Hindawi Publishing Corporation
International Journal of Antennas and Propagation
Volume 2014, Article ID 531959, 10 pages
http://dx.doi.org/10.1155/2014/531959

Research Article

Design and Analysis of a Novel Dual Band-Notched UWB Antenna

Ronghua Shi, Xi Xu, Jian Dong, and Qingping Luo

School of Information Science and Engineering, Central South University, Changsha 410075, China

Correspondence should be addressed to Jian Dong; dongjian@mail.csu.edu.cn

Received 17 April 2013; Revised 19 December 2013; Accepted 19 December 2013; Published 3 February 2014

Academic Editor: Alistair P. Duffy

A novel ultrawide band (UWB) antenna with dual band-notched characteristics is presented. The first band rejection is provided by an arc H-shaped slot on the radiating patch. The parametric study of the arc H-shaped slot shows that this structure enables rejectband characteristic with improved control compared to traditional H-shaped slot. Based on the single band-notched UWB antenna, the second notched band is realized by etching narrow slots on the ground plane. By tuning the parameters of these slots, the proposed UWB antenna can operate from 2.9 GHz to above 10 GHz, except for the bandwidth of 3.3–3.6 GHz for WiMAX application and 5.1–5.9 GHz for WLAN application. Simulated and measured results show that the proposed antenna provides excellent band rejection and is a good candidate for future UWB application.

1. Introduction

Since commercial ultrawide band (UWB) systems which work from 3.1 GHz to 10.6 GHz are allowed by Federal Communication Commission (FCC) [1], the technology of UWB is concerned by academia and industry due to its candidate for various applications. As an essential part of the UWB system, the UWB antenna, has drawn heavy attention from researchers. Due to broad bandwidth, low cost, and good radiation characteristic, the global approaches of UWB antenna [2–4] are increasing quickly.

In order to avoid interference of service that work in the UWB band, such as the subband 5.1–5.9 GHz for WLAN band and WiMAX operating in the 3.3–3.6 GHz, the UWB antenna with band-notched function is desirable. Various methods for designing band-notched UWB antenna have been presented and reported. Designs of using parasitic stubs as resonators to achieve band-notched function were presented in [5–8]. In [5], single band-notched and multiband-notched antennas have been implemented by integrating wideband planar monopole antennas with various types of microstrip resonator. In [6], band-notched function of the circle ring antenna was achieved by introducing a tuning stub inside the ring monopole. A monopole antenna with band-notched function using a complex resonator was presented in [7]. A printed monopole antenna with controllable band-notched performance for UWB applications was presented in [8]. Its band-notched characteristic is achieved by embedding two shorted rectangular resonators.

In the designs above, the structure of these antennas cannot be compact enough due to the use of parasitic stubs as resonators. In order to make the structure of the band-notched antenna more compact, etching slots such as C-shaped, T-shaped, E-shaped, and H-shaped slots on the radiating patch or on the ground plane were used to achieve band-notched function [9–15]. Designs of single band-notched UWB antennas were presented in [9–13]. In [9], the characteristics of the on-ground band-notched structures were analyzed in detail providing designers with useful information and flexibility for the realization of specialized band-notched antennas. In [10], characteristic modes have been used to analyze the behavior of an UWB antenna with a narrowband slot embedded in its planar geometry. It has been shown that the notched-band is caused by the slot resonance, and the intensity of the rejection depends on how much the current distribution of different antenna modes is disturbed. By using a modified shovel-shaped defected ground structure, a band-notched characteristic is achieved in [11]. A

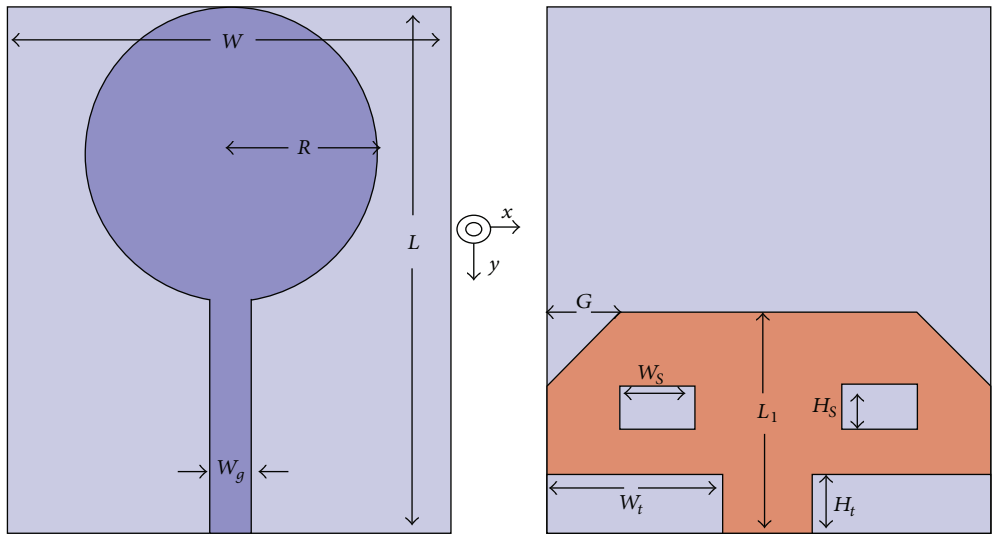

Figure 1: Geometry of the UWB antenna: (a) top view, (b) bottom view.

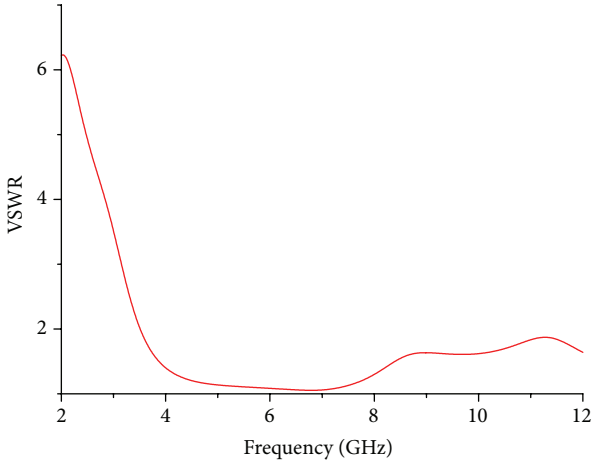

Figure 2: Simulated VSWR of the UWB antenna.

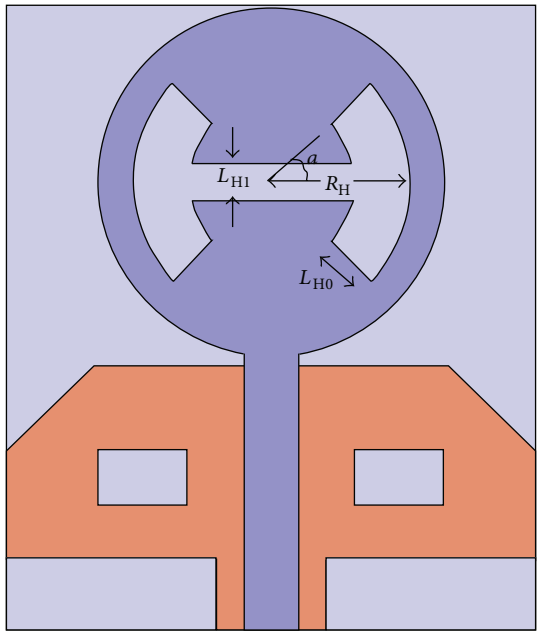

Figure 3: Geometry of the arc H-shaped slot.

frequency-reconfigurable planar antenna with two inverted S-shaped slots was presented in [12]. This antenna can be widely used in the dual-band WLAN systems and the UWB systems. In addition, a complete design method for a compact uniplanar UWB antenna with subband rejection capability is presented in [13]. In order to avoid the interference from services which work in different frequency band, dual band-notched UWB antennas were presented [14, 15]. In [14], the dual band-notched function was achieved by etching one quasi-complementary split-ring resonator in the feed line. In [15], by cutting two L-shaped slits and an E-shaped slot with variable dimensions on the radiating patch dual band-notch characteristics generated and also by inserting a V-shaped strip on the ground plane, additional resonances were excited, and hence much wider impedance bandwidth was produced, especially at the higher band.

The designed antennas above feature wide operating bandwidth and good band-notched function, but they lack powerful control of tuning the centre frequency of the notched-band. To overcome this weakness of the above designs, a novel UWB antenna with dual band-notched characteristics is proposed in this paper by employing an arc H-shaped slot on the radiating patch and etching narrow slots on the ground plane. The proposed antenna can operate within an ultrawide band from 2.9 GHz to above 10 GHz. At the same time, the antenna can avoid the interference from WiMAX and WLAN applications. The rest of the paper is organized

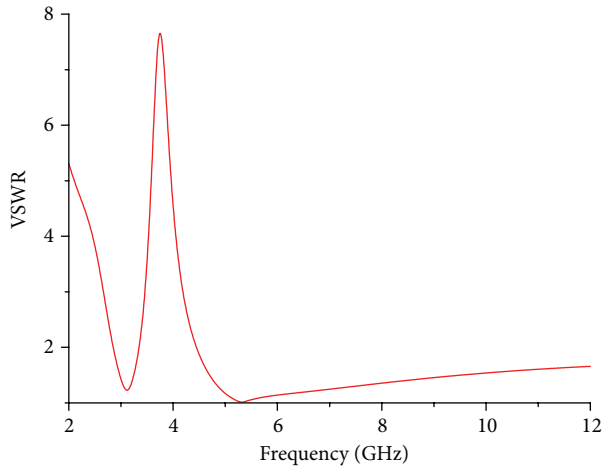

Figure 4: Simulated VSWR of the single band-notched antenna.

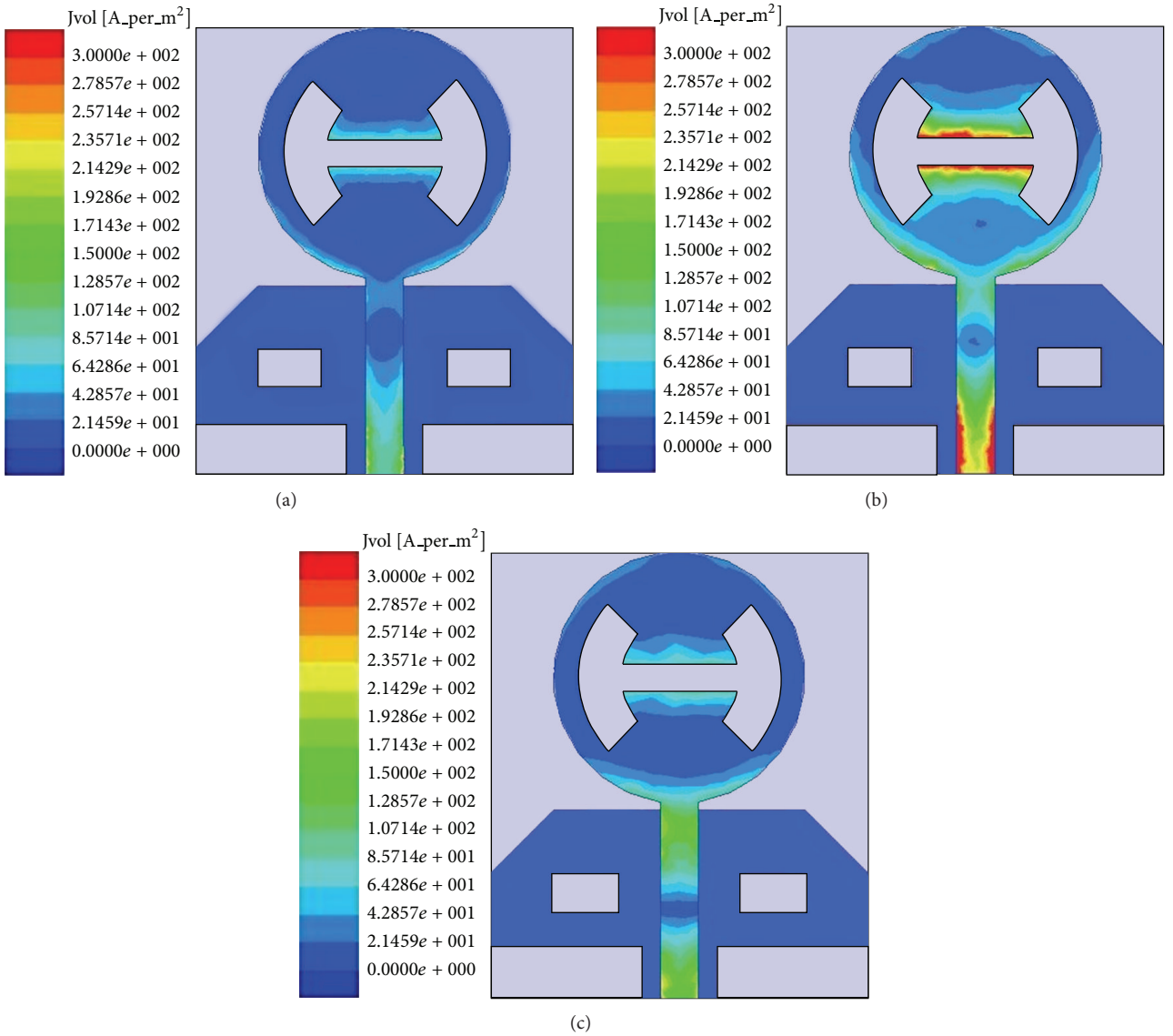

Figure 5: Surface current distribution of the antenna: (a) 3.2 GHz, (b) 3.7 GHz, and (c) 5 GHz.

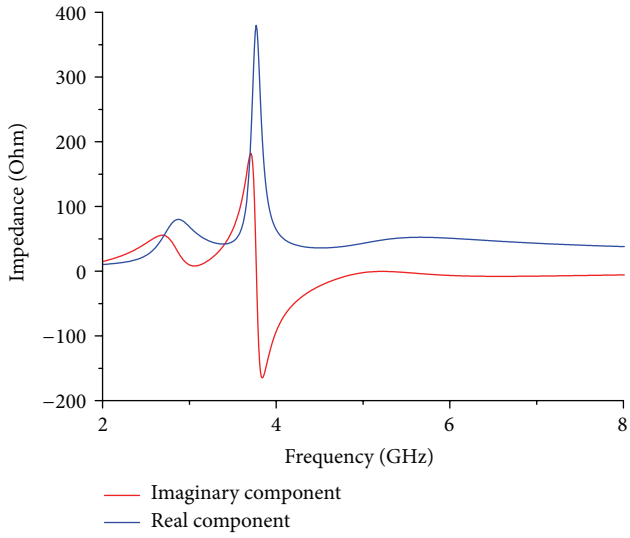

Figure 6: Impedance Z of the antenna versus frequency.

as follows. In Section 2, the antenna design is first discussed. The simulation is carried out using Ansoft High Frequency Structure Simulator (HFSS). In Section 3, advantages of the arc H-shaped slot compared with traditional H-shaped slot are presented. In Section 4, simulation and measurement results are presented to validate the performance of the proposed antenna. Finally, the conclusion is provided in Section 5.

2. Antenna Design

2.1. Single Band-Notched UWB Antenna Design

2.1.1. UWB Antenna. As shown in Figure 1. The referance antenna [4] uses FR4 substrate with the dimensions of $35.5 \times 30 \times 1.6\ \text{mm}^3$, relative permittivity $\varepsilon_r = 4.4$. The antenna is fed by a CPW line which is designed for 50 Ohm characteristic impedance. Figure 1(a) shows the top view of the antenna; the planar circular disc monopole is fabricated on the substrate. The radius of the radiating patch is R (R = 10 mm), and the width of the feed line is W_g (W_g = 3 mm). Figure 1(b) shows the rear of the antenna; the length of the ground plane is L_1 (L_1 = 15 mm). The top corners with the parameter G (G = 5 mm) are removed to improve the bandwidth of the antenna [4]. Two rectangular slots are removed to adjust the antenna impedance and reduce the return loss [4]. H_s (H_s = 3 mm) and W_s (W_s = 5 mm) denote the length and width of the rectangular slots, respectively. The ground plane is reshaped as letter "T", for W_t = 12 mm, H_t = 4 mm. The simulated VSWR result of the UWB antenna is shown in Figure 2; it can be seen that the antenna could operate from 3.5 GHz to above 12 GHz with VSWR less than 2.

2.1.2. Single Band-Notched UWB Antenna. Before developing the dual band-notched UWB antennas, we need to investigate the method generating the single notched band. In order to achieve band-notched function, we employ an arc H-shaped slot on the circular radiating patch. The arc H-shaped slot is removed from the centre of the radiating patch. As shown in Figure 3, the shape of the slot is designed as an arc letter "H." R_{H} denotes the radius of the outer circular arc. L_{H0} denotes the distance between outer arc and inner arc. The simulation is carried out using HFSS. The optimized slot dimensions are as follows: $R_{\text{H}} = 8$ mm, $L_{\text{H0}} = 3.2$ mm, $L_{\text{H1}} = 2$ mm, and $\alpha = \pi/4$. It can be seen in Figure 4 that the simulated VSWR of the antenna is larger than 2 from 3.2 GHz to 4.2 GHz acting as a stopband, meaning that this antenna can avoid the interference from IEEE 802.16 WiMAX application.

The simulated results of surface current distribution for the antenna at the passband (3.2 GHz, 5 GHz) and at the rejectband (3.7 GHz) are given in Figure 5. It can be seen that the surface current distribution is very strong at the feed line and the surface current is highly concentrated at the arc H-shaped slot in Figure 5(b), but the situations are different in Figures 5(a) and 5(c). These clearly show the positive effects of the slot upon obtaining the band-notched characteristics. It is noted that the UWB antenna cannot work at the stopband (3.7 GHz) because of the effect of the arc H-shaped slot resonator. The impedance Z of the antenna versus frequency is given in Figure 6 to show the band-notched function of this antenna. The input resistance should be around 50 Ohm and the input reactance should be around 0 Ohm when the antenna is operating at the passband. At the stopband, their values largely deviate from the nominal values.

2.2. Dual Band-Notched UWB Antenna Design. The high frequency band-notched function is designed to avoid the other band such as WLAN operating from 5.1 to 5.9 GHz. To achieve this function, we etch a couple of narrow slots on the ground plane. Figure 7 shows the geometry of the antenna; the top view of this antenna and the slots on the ground plane are given in Figures 7(a) and 7(b), respectively. The simulated results show that the optimized slot dimensions are as follows: $W_d = 0.5$ mm, $L_d = 7.5$ mm, and $S = 0.2$ mm. The VSWR result is shown in Figure 8; it can be seen that the antenna could not operate from 5.1 GHz to 6 GHz as a stopband. The centre frequency of the stopband, given the dimensions of the band-notched feature, can be postulated as [16]

$$f_{\text{notch}} = \frac{c}{4L'\sqrt{(\varepsilon_r + 1)/2}}. \tag{1}$$

Let $L' = L_d + W_d$; ε_r is the effective dielectric constant, and c is the speed of light. The lengths of the slot have great effects on the band rejection performance and should be tuned carefully. By varying the length of parameter L_d, we could control the length of L' to tune the centre frequency of the stopband.

Based on the single band-notched UWB antenna, the dual band-notched function is investigated, and the geometry of the antenna is given in Figure 9. Figure 10 shows the simulated VSWR result of the dual band-notched UWB antennap; it can be observed that the proposed antenna bandwidth with good stopband rejection, the band-notched characteristic of low frequency formed by the arc H-shaped slot on the radiating patch, and the band-notched characteristic of high

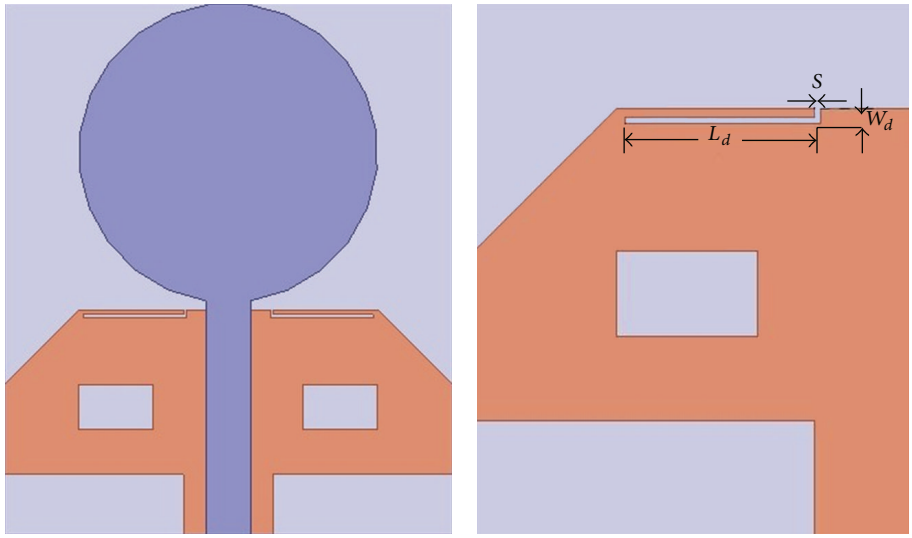

Figure 7: Geometry of the high frequency band-notched antenna: (a) top view, (b) narrow slot on the ground plane.

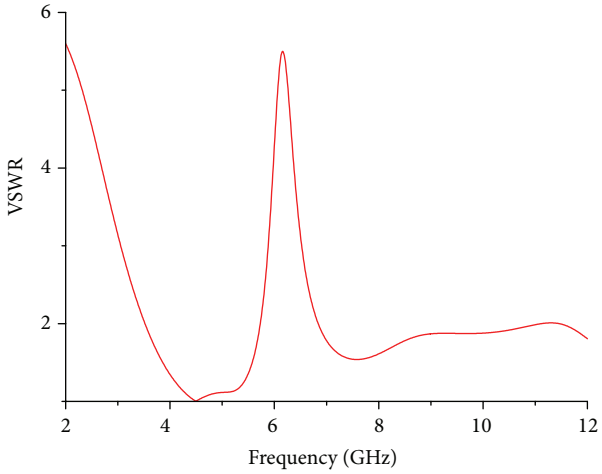

Figure 8: Simulated VSWR of the high frequency band-notched UWB antenna.

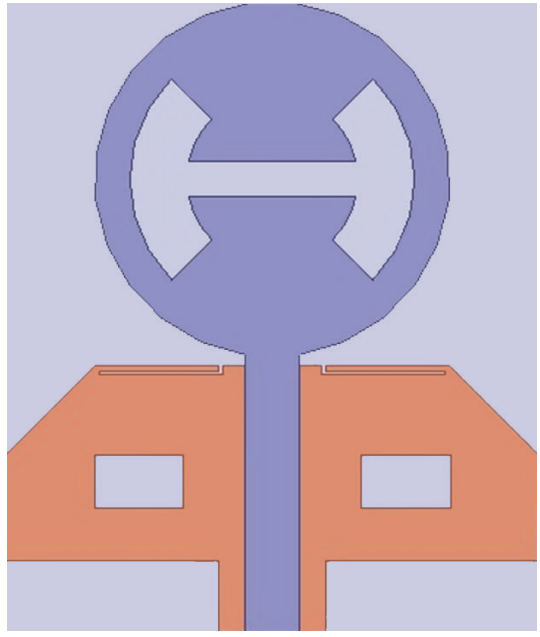

Figure 9: Geometry of the proposed antenna.

frequency formed by the narrow slots on the ground plane hardly interfere with each other. Figure 11 shows that the centre frequency of the stopband shifts down as L_d increases. The impedance Z of the dual band-notched UWB antenna is displayed in Figure 12, which shows that the input resistance and the input reactance keep the nominal value when the antenna working on the passband. It shows that the proposed antenna is suitable for UWB applications.

According to the impedance Z of the dual band-notched UWB antenna shown in Figure 12, the approximate equivalent circuit of the proposed antenna is presented in Figure 13. The arc H-shaped slot on the radiating patch and narrow slots on the ground plane can be modeled by two circuit-resonance stubs at different positions in a transmission line model. At the passband, neither of the stubs has any effect in generating notched bands. On the 3.7 GHz band-notched characteristic, stub 1 makes the circuit resonate. Therefore, stub 1 behaves as a parallel resonator with an unusual input impedance Z (i.e., the input resistance is much larger than 50 Ohm, and the input reactance is not equal to 0 Ohm), causing a total impedance mismatch between the feed line and the radiating patch. As a result, VSWR of the antenna in this frequency band becomes greater, and the first notched band is created. On the 5.7 GHz band-notched characteristic, stub 2 works similarly as stub 1. The input impedance Z becomes unusual; stub 2 operates as a parallel resonator in

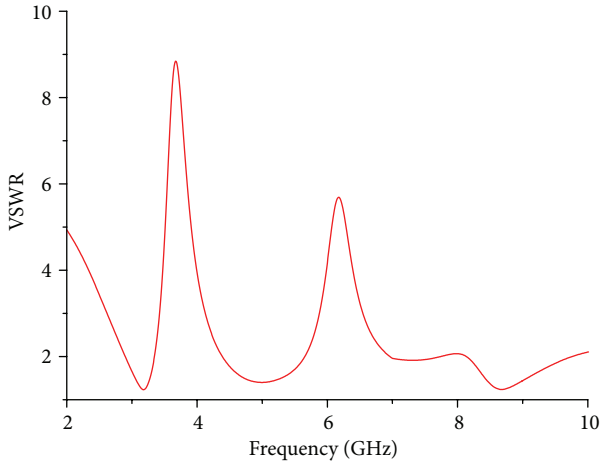

Figure 10: Simulated VSWR result of the proposed antenna.

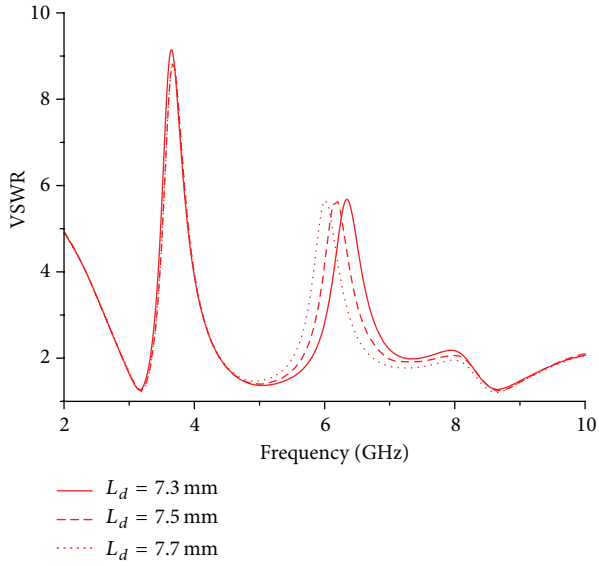

Figure 11: Effect of length of the narrow slot.

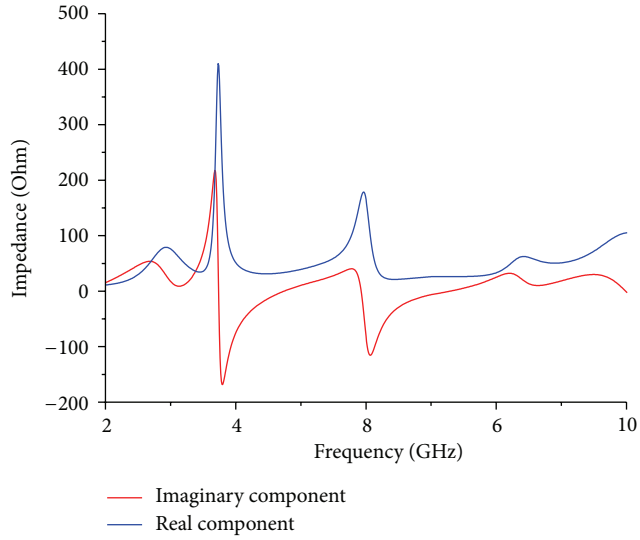

Figure 12: Impedance Z of the proposed antenna versus frequency.

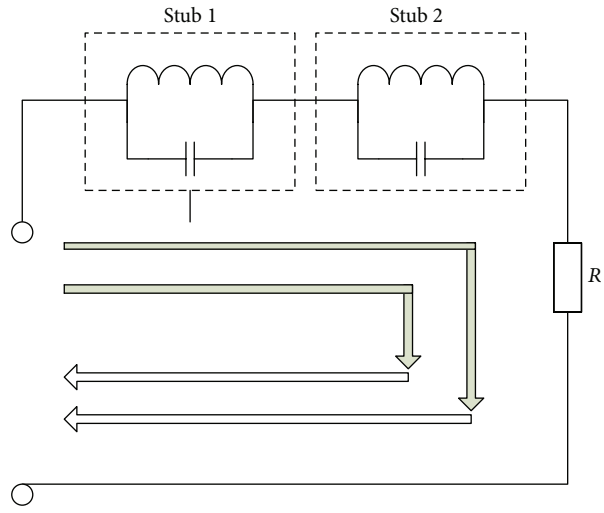

Figure 13: Approximate equivalent circuit of the proposed antenna.

the circuit. Essentially, the dual band-notched function is achieved by these resonators.

3. Advantages of the Arc H-Shaped Slot

Traditional H-shaped slot is designed as follows. The geometry and parameters of the H-shaped slot are shown in Figure 14. Through the parametric study [17], the effects of H-shaped slot parametric variation on stopband centre frequency are presented in Table 1 [17]. It can be seen that stopband centre frequency can be tuned effectively only by varying parameter W_{S1}.

In the proposed antenna, the first rejectband centre frequency is mainly determined by the dimensions of the parameters of the arc H-shaped slot. In order to show the advantages of the arc H-shaped slot, the parametric effects

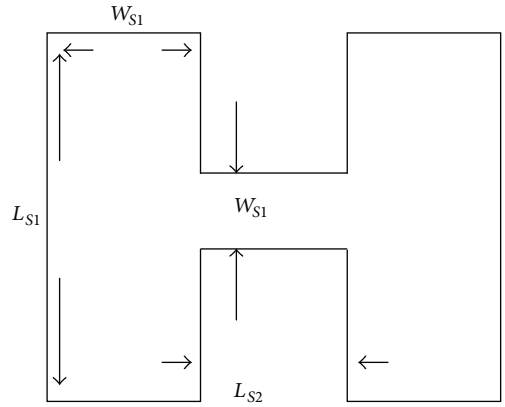

Figure 14: geometry and parameters of the H-shaped slot.

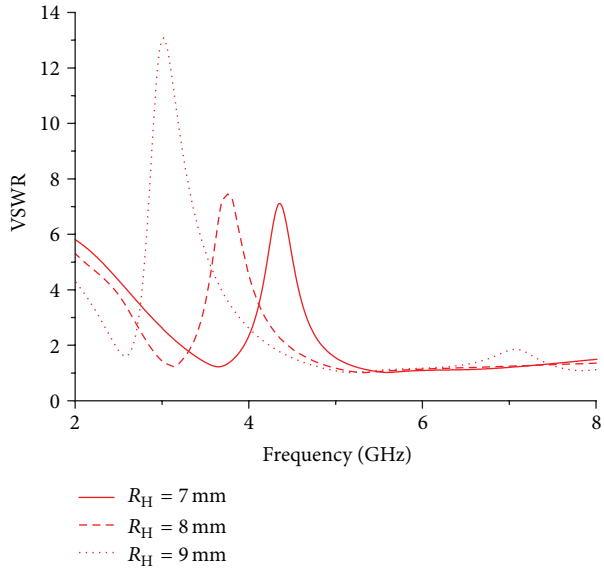

Figure 15: Effect of parameter R_H.

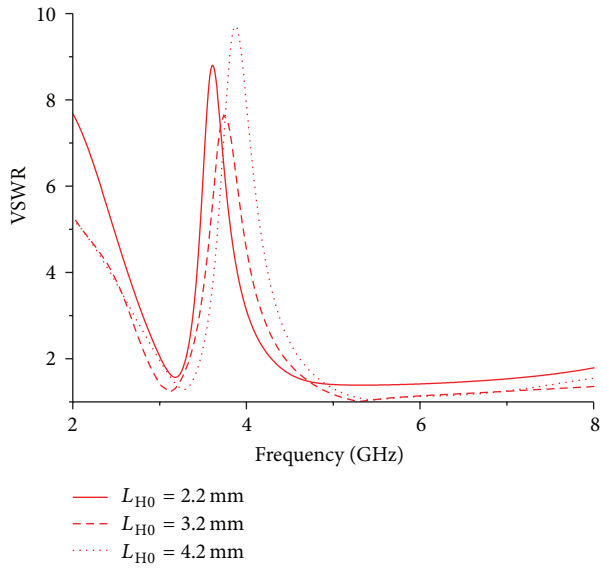

Figure 16: Effect of parameter L_{H0}.

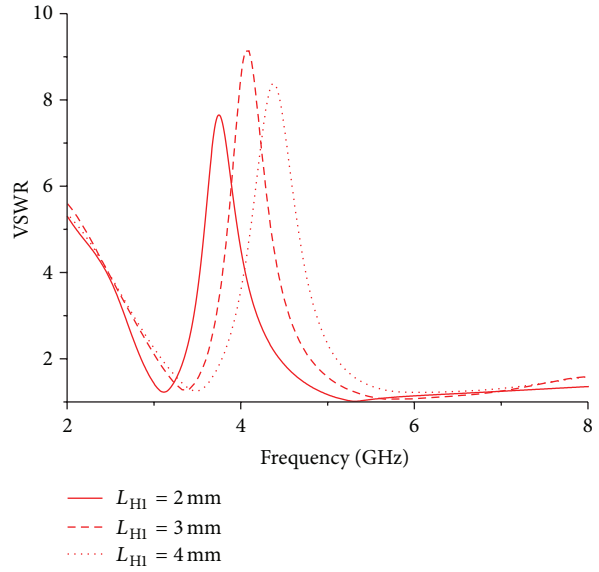

Figure 17: Effect of parameter L_{H1}.

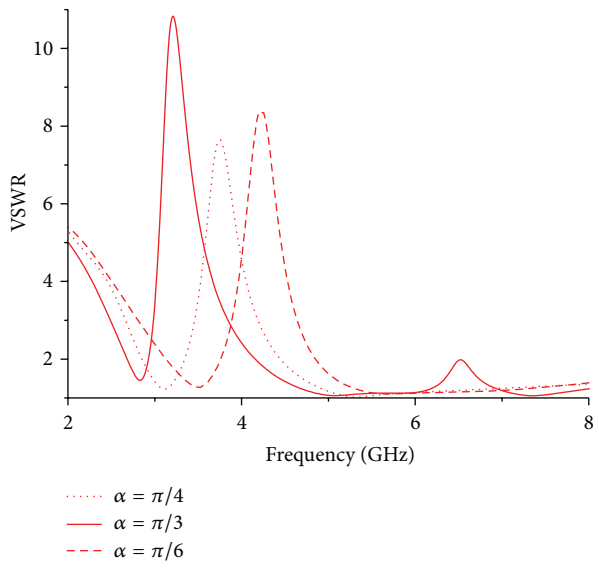

Figure 18: Effect of parameter angle α.

(R_H, L_{H0}, L_{H1}, and α) of the slot are analyzed to show the advantages of the novel design.

On the 3.7 GHz band-notched characteristic, the effect of parameter R_H is simulated and shown in Figure 15. The dimensions of the arc H-shaped slot are L_{H0} = 3.2 mm, L_{H1} = 2 mm, and $\alpha = \pi/4$; we can be informed that centre frequency of the band changes from 3.2 GHz to 4.4 GHz when parameter R_H varies from 7 mm to 9 mm. It can be seen that the centre frequency of the stopband shifts down as R_H increases. The notch frequency is heavily dependent on this parameter.

The slot dimension L_{H0}, varies, for R_H = 8 mm, L_{H1} = 2 mm, and $\alpha = \pi/4$. The simulated VSWR of Figure 16 shows that frequency band notch varied from 3.7 GHz to 4 GHz as L_{H0} increases. Relatively, the notch frequency shows light dependence on L_{H0}.

Figure 17 shows the simulated VSWR of the effect of parameter L_{H1}. It can be seen that the centre frequency varies from 3.6 GHz to 4.6 GHz as L_{H1} varies from 2 mm to 4 mm. The simulated VSWR in Figures 16 and 17 illustrate that the slot dimension L_{H0} has a smaller effect on notch frequency than the parameter L_{H1}. It can be informed that the centre frequency is heavily dependent on parameter L_{H1} (R_H = 8 mm, L_{H0} = 3.2 mm, and $\alpha = \pi/4$).

In addition, another important parameter α is analyzed below. The effect of angle α is simulated and shown in Figure 18. The slot dimension α, varies, for R_H = 8 mm, L_{H0} = 3.2 mm, and L_{H1} = 2 mm. It can be seen that the centre

Figure 19: Photograph of the proposed antenna.

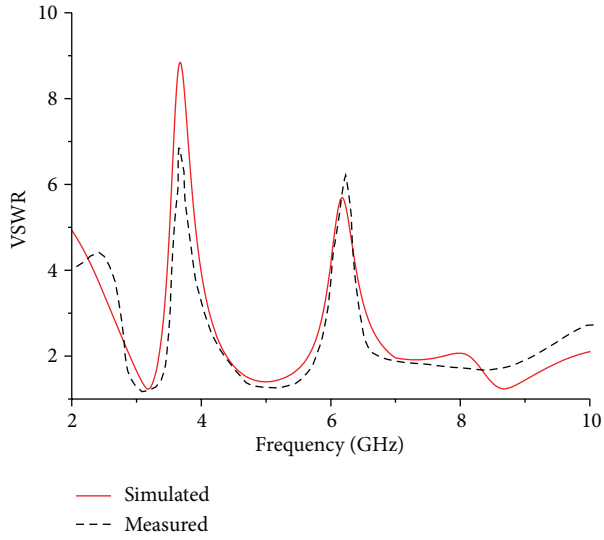

Figure 20: Simulated and measured VSWR results of the proposed antenna.

frequency of the stopband changes from 3.2 GHz to 4.5 GHz as angle α varies from $\pi/6$ to $\pi/3$. The simulated results show that a large shift in notch frequency took place with no other significant changes, so angle α is also one of the most important factors of tuning the centre frequency.

In conclusion, the effects of arc H-slot parametric variation on stopband centre frequency are presented in Table 2. It can be seen that the band-notched frequency is heavily dependent on parameters R_H, L_{H1}, and angle α and is lightly dependent on parameter L_{H0}. It can be easy to observe that the notch frequency can be tuned efficiently by changing any parameter except L_{H0}. Relative to the conventional H-shaped slot which can only change the length of the parameter W_{S1} [17], the desirable notch frequency can be achieved by varying one or more parameters of the arc H-shaped slot. Due to the characteristics of the arc H-shaped slot, the antenna provides easier tuning of the band-notched function. Through the analysis of the parameters of the arc H-shaped slot, advantages of the proposed antenna are presented.

Table 1: The effects of H-shaped slot parametric variation on stopband centre frequency [17].

Parameters	Stopband centre frequency
L_{S1}	Light dependence
L_{S2}	Light dependence
W_{S1}	Heavy dependence
W_{S2}	No dependence

Table 2: The effects of Arc H-shaped slot parametric variation on stopband centre frequency.

Parameters	Centre frequency changes per 2 mm	Stopband centre frequency
R_H	1.2 GHz	Heavy dependence
L_{H0}	0.3 GHz	Light dependence
L_{H1}	1 GHz	Heavy dependence
α	1.3 GHz (α varied from $\pi/6$ to $\pi/3$)	Heavy dependence

4. Results and Discussion

The photograph of fabricated dual band-notched UWB antenna is shown in Figure 19. A rectangular finite FR4 board is used for manufacture. The circular radiating patch is supported by an SMA connector. Figure 20 shows the simulated and measured VSWR results of the dual band-notched UWB antenna, it can be seen that the measured VSWR agrees well with the simulated result. The fabricated antenna covers the frequency range for UWB systems from 2.9 GHz to above 10 GHz with rejection bands around 3.3–4.2 GHz and 5.2–5.9 GHz. The discrepancy between the simulated and measured results could be mainly due to errors in processing and effect of the SMA connector. In order to confirm the accurate VSWR for the designed antenna, it is recommended that the manufacturing and measuring process should be performed carefully.

The antenna is usually required to have an omnidirectional radiation concerning the UWB applications. The simulated and measured radiation patterns at 3.2 GHz, 5 GHz, and 8 GHz are illustrated in Figures 21(a), 21(b), and 21(c); we can see that the measurements and the simulations show good agreement. The main purpose of these radiation patterns is to demonstrate that the antenna actually radiates over a wide frequency band. At the passband frequencies out of the notched bands, the antenna needs to have good omnidirectional radiation patterns. As shown in the figure, the radiation patterns in the yz-plane look like an "8" shape and in the xz-plane they are nearly round-shaped. It is noted that the proposed antenna gives nearly omnidirectional radiation patterns in the H-plane (xz-plane) and E-plane (yz-plane) at the passband.

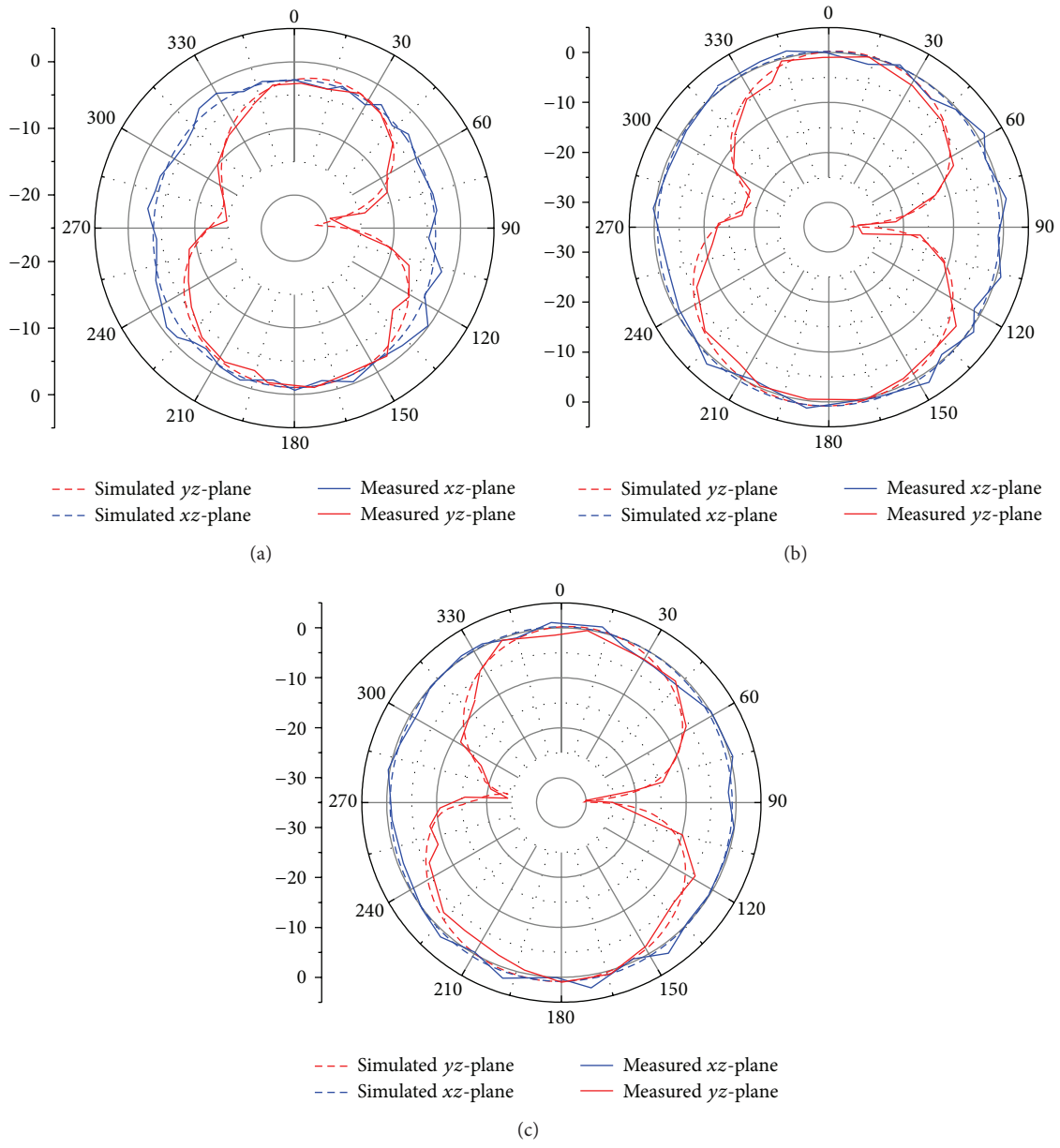

Figure 21: Measured and simulated radiation patterns of the proposed antenna: (a) 3.2 GHz, (b) 5 GHz, and (c) 8 GHz.

In addition, the total efficiency versus frequency of the proposed antenna is given in Figure 22. The proposed antenna should exhibit two sharp efficiency decreases at 3.7 GHz and 5.6 GHz. According to the figure, the range of the measurements is from 3 GHz to 10 GHz; the efficiency decreases sharply at the notched frequency band because of the resonators of the proposed antenna. At the passband, the efficiency remains at high level. It is clear from the results that the antenna cannot operate at the rejectband and can work efficiently at the passband.

5. Conclusions

A novel UWB antenna with dual band-notched function has been proposed and analyzed in this paper. The primitive UWB antenna is fabricated on a FR4 substrate. An arc H-shaped slot etched on the radiating patch and narrow slots etched on the ground plane are used to achieve the dual band-notched function. The parameters of the arc H-shaped slot are analyzed to show the advantages of the proposed antenna which provides improved control of tuning the centre frequency of the rejectband. The bandwidth of the low frequency band-notched antenna formed by the arc H-shaped slot and the bandwidth of the high frequency band-notched antenna formed by the narrow slots do not interfere with each other. The results of surface current distributions and the input impedance show that the designed antenna bandwidth with good band rejection is presented. Nearly omnidirectional radiation patterns and desirable efficiency of the antenna which could be observed by the simulated and

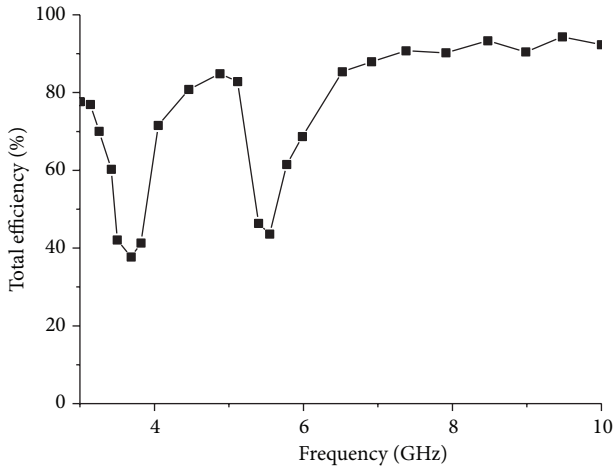

Figure 22: Total efficiency versus frequency.

measured results are also presented to verify the satisfactory performance of the proposed antenna.

Conflict of Interests

The authors declare that there is no conflict of interests regarding the publication of this paper.

Acknowledgments

This work was supported in part by the National Science Foundation of China under Grant NSFC61201086 and Grant NSFC61101235, the Doctoral Fund of Ministry of Education of China under Grant 20110162120044, and China Postdoctoral Science Foundation under Grant no. 2012T50660.

References

[1] Federal Communications Commission, *First Report and Order in the Matter of Revision of Part 1-5 of the Commission Rules Regarding Ultra-Wideband Transmission Systems*, 2002.

[2] T. Aboufoul and A. Alomainy, "Reconfigurable printed UWB circular disc monopole antenna," in *Proceedings of the 7th Loughborough Antennas and Propagation Conference (LAPC '11)*, Loughborough, November 2011.

[3] T. Aboufoul and A. Alomainy, "Single-element reconfigurable planar ultra wideband antenna for cognitive radio front end," in *Proceedings of the 4th International Conference on Cognitive Radio and Advanced Spectrum Management (CogART '11)*, Barcelona, Spain, October 2011.

[4] N. Prombutr, P. Kirawanich, and P. Akkaraekthalin, "Bandwidth enhancement of UWB microstrip antenna with a modified ground plane," *International Journal of Microwave Science and Technology*, vol. 2009, Article ID 821515, 7 pages, 2009.

[5] D.-Z. Kim, W.-I. Son, W.-G. Lim, H.-L. Lee, and J.-W. Yu, "Integrated planar monopole antenna with microstrip resonators having band-notched characteristics," *IEEE Transactions on Antennas and Propagation*, vol. 58, no. 9, pp. 2837–2842, 2010.

[6] S. Ghosh, "Band-notched modified circular ring monopole antenna for ultrawideband applications," *IEEE Antennas and Wireless Propagation Letters*, vol. 9, pp. 276–279, 2010.

[7] S.-J. Wu, C.-H. Kang, K.-H. Chen, and J.-H. Tarng, "Study of an ultrawideband monopole antenna with a band-notched open-looped resonator," *IEEE Transactions on Antennas and Propagation*, vol. 58, no. 6, pp. 1890–1897, 2010.

[8] A. Ghobadi, C. Ghobadi, and J. Nourinia, "A novel band-notched planar monopole antenna for ultrawideband applications," *IEEE Antennas and Wireless Propagation Letters*, vol. 9, pp. 608–611, 2010.

[9] Y. D. Dong, W. Hong, Z. Q. Kuai, and J. X. Chen, "Analysis of planar ultrawideband antennas with on-ground slot band-notched structures," *IEEE Transactions on Antennas and Propagation*, vol. 57, no. 7, pp. 1886–1893, 2009.

[10] E. Antonino-Daviu, M. Cabedo-Fabrés, M. Ferrando-Bataller, and V. M. R. Peñarrocha, "Modal analysis and design of band-notched UWB planar monopole antennas," *IEEE Transactions on Antennas and Propagation*, vol. 58, no. 5, pp. 1457–1467, 2010.

[11] A. Nouri and G. R. Dadashzadeh, "A compact UWB band-notched printed monopole antenna with defected ground structure," *IEEE Antennas and Wireless Propagation Letters*, vol. 10, pp. 1178–1181, 2011.

[12] B. Li, J. S. Hong, and B. Z. Wang, "Switched band-notched UWB/dual-band WLAN slot antenna with inverted S-shaped slots," *IEEE Antennas and Wireless Propagation Letters*, vol. 11, pp. 572–575, 2012.

[13] A. M. Abbosh, "Design of a CPW-fed band-notched UWB antenna using a feeder-embedded slotline resonator," *International Journal of Antennas and Propagation*, vol. 2008, Article ID 564317, 5 pages, 2008.

[14] W. T. Li, Y. Q. Hei, W. Feng, and X. W. Shi, "Planar antenna for 3G/Bluetooth/WiMAX and UWB applications with dual band-notched characteristics," *IEEE Antennas and Wireless Propagation Letters*, vol. 11, pp. 61–64, 2012.

[15] M. Mehranpour, J. Nourinia, C. Ghobadi, and M. Ojaroudi, "Dual band-notched square monopole antenna for ultrawideband applications," *IEEE Antennas and Wireless Propagation Letters*, vol. 11, pp. 172–175, 2012.

[16] L.-H. Ye and Q.-X. Chu, "3.5/5.5GHz dual band-notch ultrawideband slot antenna with compact size," *Electronics Letters*, vol. 46, no. 5, pp. 325–327, 2010.

[17] X. L. Bao and M. J. Ammann, "Printed UWB antenna with coupled slotted element for notch-frequency function," *International Journal of Antennas and Propagation*, vol. 2008, Article ID 713921, 8 pages, 2008.